

Supporting Information

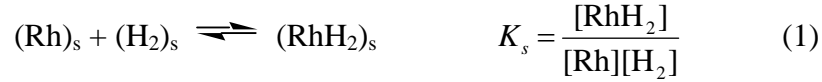
Transition State Characterization for the Reversible Binding of Dihydrogen to Bis(2,2'-bipyridine)rhodium(I) from Temperature- and Pressure-Dependent Experimental and Theoretical Studies

Etsuko Fujita, Bruce S. Brunschwig, Carol Creutz, James T. Muckerman, Norman Sutin, David Szalda, and Rudi van Eldik

Chemistry Department, Brookhaven National Laboratory, Upton, New York 11973-5000, USA
and Institute for Inorganic Chemistry, University of Erlangen-Nürnberg, Egerlandstr. 1, 91058
Erlangen, Germany

Conversion of the standard state of hydrogen:

The relevant equilibria are



Where the square brackets denote equilibrium concentrations in solution and P_{H_2} is the partial pressure of hydrogen above the solution. Thus

$$K_p = K_s K_{sp} \text{ and } \Delta G_p^0 = \Delta G_s^0 + \Delta G_{sp}^0 \quad (4)$$

and

$$\Delta G_{sp}^0 = -RT \ln \left(\frac{[\text{H}_2]}{P_{\text{H}_2}} \right) \quad (5)$$

From Henry's law

$$P_{\text{H}_2} = k_H [\text{H}_2] \quad (6)$$

where k_H is the Henry's law constant. k_H is equal to the inverse of the concentration of hydrogen at 1 atmosphere of H_2 pressure. Thus we get

$$\Delta G_{sp}^0 = -RT \ln \left(\frac{[\text{H}_2]}{P_{\text{H}_2}} \right) = -RT \ln \left(\frac{1}{k_H} \right) = -RT \ln(m_s) \quad (7)$$

where m_s is the solubility of hydrogen at STP. Now

$$\Delta G_{sp}^0 = \Delta H_{sp}^0 - T \Delta S_{sp}^0 \quad (8)$$

where

$$\Delta H_{sp}^0 = \left(\frac{\partial (\Delta G_{sp}^0 / T)}{\partial (1/T)} \right)_p \quad (9)$$

$$\Delta S_{sp}^0 = - \left(\frac{\partial \Delta G_{sp}^0}{\partial T} \right)_p = - \frac{\Delta G_{sp}^0 - \Delta H_{sp}^0}{T} \quad (10)$$

Thus we obtain

$$\Delta G_c^0 = \Delta G_p^0 - \Delta G_{sp}^0 \quad (11a)$$

$$\Delta H_c^0 = \Delta H_p^0 - \Delta G_{sp}^0 \quad (11b)$$

$$\Delta S_c^0 = \Delta S_p^0 - \Delta S_{sp}^0 \quad (11c)$$

From data on the solubility of
H₂ as a function of 1/T at 1 atmosphere
pressure in methanol we obtain

$$\Delta G_{sp}^0 = 3.3 \text{ kcal mol}^{-1}$$

$$\Delta H_{sp}^0 = 0.62 \text{ kcal mol}^{-1}$$

$$\Delta S_{sp}^0 = -8.9 \text{ cal mol}^{-1} \text{ K}^{-1}$$

Similarly in acetone, we obtain

$$\Delta G_{sp}^0 = 3.2 \text{ kcal mol}^{-1}$$

$$\Delta H_{sp}^0 = 0.95 \text{ kcal mol}^{-1}$$

$$\Delta S_{sp}^0 = -7.7 \text{ cal mol}^{-1} \text{ K}^{-1}$$

Using these values in eqs 11b
and 11c we obtain the correction
needed.

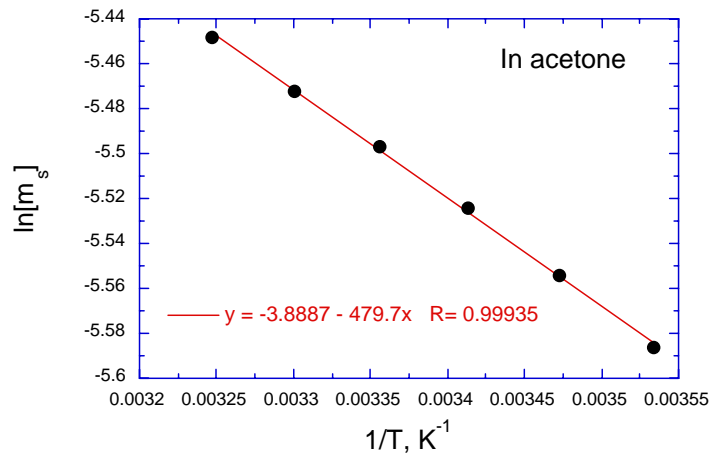
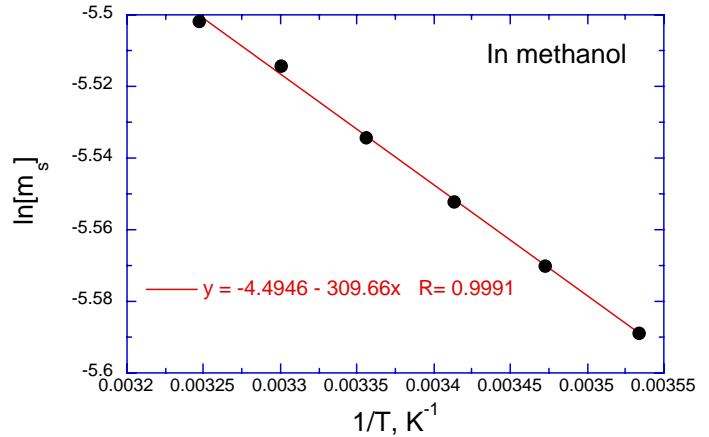


Table S1. The Cartesian Coordinates for Rh(bpy)₂⁺ optimized the DFT-B3LYP Level Theory in Methanol

Rh	0. 0000000000	0. 0000000000	0. 0000000000
C	-1. 5381575867	2. 5360130401	0. 7961503817
N	-1. 6263393922	1. 2814812387	0. 3052561149
C	-2. 8589051811	0. 6967286119	0. 2365342598
C	-4. 0136358716	1. 3821881689	0. 6254262592
C	-3. 9122963414	2. 6870309674	1. 1024846571
C	-2. 6488150281	3. 2712821688	1. 1970854769
N	-1. 6263393922	-1. 2814812387	-0. 3052561149
C	-1. 5381575867	-2. 5360130401	-0. 7961503817
C	-2. 6488150281	-3. 2712821688	-1. 1970854769
C	-3. 9122963414	-2. 6870309674	-1. 1024846571
C	-4. 0136358716	-1. 3821881689	-0. 6254262592
C	-2. 8589051811	-0. 6967286119	-0. 2365342598
H	-4. 9807883821	0. 8948211725	0. 5770496563
H	-4. 8017762499	3. 2283270275	1. 4101752591
H	-2. 5129815515	4. 2767684457	1. 5815971008
H	-0. 5418949520	2. 9514399772	0. 8833874582
H	-2. 5129815515	-4. 2767684457	-1. 5815971008
H	-4. 8017762499	-3. 2283270275	-1. 4101752591
H	-4. 9807883821	-0. 8948211725	-0. 5770496563
H	-0. 5418949520	-2. 9514399772	-0. 8833874582
C	1. 5381575867	-2. 5360130401	0. 7961503817
N	1. 6263393922	-1. 2814812387	0. 3052561149
C	2. 8589051811	-0. 6967286119	0. 2365342598
C	4. 0136358716	-1. 3821881689	0. 6254262592
C	3. 9122963414	-2. 6870309674	1. 1024846571
C	2. 6488150281	-3. 2712821688	1. 1970854769
N	1. 6263393922	1. 2814812387	-0. 3052561149
C	1. 5381575867	2. 5360130401	-0. 7961503817
C	2. 6488150281	3. 2712821688	-1. 1970854769
C	3. 9122963414	2. 6870309674	-1. 1024846571
C	4. 0136358716	1. 3821881689	-0. 6254262592
C	2. 8589051811	0. 6967286119	-0. 2365342598
H	4. 9807883821	-0. 8948211725	0. 5770496563
H	4. 8017762499	-3. 2283270275	1. 4101752591
H	2. 5129815515	-4. 2767684457	1. 5815971008
H	0. 5418949520	-2. 9514399772	0. 8833874582
H	2. 5129815515	4. 2767684457	-1. 5815971008

H	4. 8017762499	3. 2283270275	-1. 4101752591
H	4. 9807883821	0. 8948211725	-0. 5770496563
H	0. 5418949520	2. 9514399772	-0. 8833874582

Table S2. The Cartesian Coordinates for Rh(H)₂(bpy)₂⁺ optimized the DFT-B3LYP Level Theory in Methanol

Rh	0. 0000000000	0. 0000000000	0. 7572758290
C	-1. 7136117486	2. 3932916442	1. 4958342039
N	-1. 6587797197	1. 2561666974	0. 7729242421
C	-2. 7610698677	0. 8369918643	0. 0916098861
C	-3. 9515144253	1. 5714714482	0. 1504526695
C	-4. 0094796455	2. 7395058829	0. 9070738853
C	-2. 8682165927	3. 1634910136	1. 5872595798
N	-1. 3923174504	-0. 9963260188	-0. 6646156887
C	-1. 1868846915	-2. 1395736633	-1. 3340486532
C	-2. 1963398936	-2. 7821824210	-2. 0484549436
C	-3. 4670736003	-2. 2055228644	-2. 0654297872
C	-3. 6823077835	-1. 0113583733	-1. 3795856616
C	-2. 6212529351	-0. 4212932702	-0. 6810221175
H	-4. 8312939679	1. 2351308082	-0. 3844569811
H	-4. 9337945777	3. 3065266037	0. 9635111890
H	-2. 8636604887	4. 0665523563	2. 1887888314
H	-0. 8079030654	2. 6721014755	2. 0194708056
H	-1. 9848782432	-3. 7106745874	-2. 5686467195
H	-4. 2851678679	-2. 6773864128	-2. 6021593800
H	-4. 6671125830	-0. 5581084709	-1. 3851249027
H	-0. 1833206734	-2. 5510312078	-1. 2846224914
C	1. 7136117486	-2. 3932916442	1. 4958342039
N	1. 6587797197	-1. 2561666974	0. 7729242421
C	2. 7610698677	-0. 8369918643	0. 0916098861
C	3. 9515144253	-1. 5714714482	0. 1504526695
C	4. 0094796455	-2. 7395058829	0. 9070738853
C	2. 8682165927	-3. 1634910136	1. 5872595798
N	1. 3923174504	0. 9963260188	-0. 6646156887
C	1. 1868846915	2. 1395736633	-1. 3340486532
C	2. 1963398936	2. 7821824210	-2. 0484549436
C	3. 4670736003	2. 2055228644	-2. 0654297872
C	3. 6823077835	1. 0113583733	-1. 3795856616
C	2. 6212529351	0. 4212932702	-0. 6810221175
H	4. 8312939679	-1. 2351308082	-0. 3844569811
H	4. 9337945777	-3. 3065266037	0. 9635111890
H	2. 8636604887	-4. 0665523563	2. 1887888314
H	0. 8079030654	-2. 6721014755	2. 0194708056
H	1. 9848782432	3. 7106745874	-2. 5686467195
H	4. 2851678679	2. 6773864128	-2. 6021593800

H	4. 6671125830	0. 5581084709	-1. 3851249027
H	0. 1833206734	2. 5510312078	-1. 2846224914
H	0. 7288543062	0. 7621683649	1. 8974369198
H	-0. 7288543062	-0. 7621683649	1. 8974369198

Table S3. The Cartesian Coordinates for the transition-state complex optimized the DFT-B3LYP Level Theory in Methanol

Rh	0. 0000000000	0. 0000000000	0. 6846994305
C	-1. 6729817397	2. 4608151098	1. 2006655881
N	-1. 6530181648	1. 2414540152	0. 6229722140
C	-2. 7679087284	0. 7856892037	-0. 0188780941
C	-3. 9192252736	1. 5803906698	-0. 0920184878
C	-3. 9311620035	2. 8414200739	0. 4971532096
C	-2. 7872350275	3. 2904399649	1. 1606971247
N	-1. 5040272554	-1. 2253414308	-0. 3445607368
C	-1. 3527471778	-2. 4803292557	-0. 8069688439
C	-2. 3445475349	-3. 1478121583	-1. 5177530150
C	-3. 5500482865	-2. 4866151963	-1. 7666520796
C	-3. 7166084691	-1. 1885744666	-1. 2916831372
C	-2. 6776226893	-0. 5760680440	-0. 5781772567
H	-4. 8043705350	1. 2149816705	-0. 5993941502
H	-4. 8225115648	3. 4592890615	0. 4436057036
H	-2. 7503704492	4. 2618242332	1. 6429532484
H	-0. 7622993337	2. 7608242917	1. 7083047456
H	-2. 1687041422	-4. 1606857320	-1. 8659933338
H	-4. 3479118764	-2. 9720418794	-2. 3204360291
H	-4. 6454386403	-0. 6613198529	-1. 4775130625
H	-0. 4014662786	-2. 9579587183	-0. 5968820181
C	1. 6729817397	-2. 4608151098	1. 2006655881
N	1. 6530181648	-1. 2414540152	0. 6229722140
C	2. 7679087284	-0. 7856892037	-0. 0188780941
C	3. 9192252736	-1. 5803906698	-0. 0920184878
C	3. 9311620035	-2. 8414200739	0. 4971532096
C	2. 7872350275	-3. 2904399649	1. 1606971247
N	1. 5040272554	1. 2253414308	-0. 3445607368
C	1. 3527471778	2. 4803292557	-0. 8069688439
C	2. 3445475349	3. 1478121583	-1. 5177530150
C	3. 5500482865	2. 4866151963	-1. 7666520796
C	3. 7166084691	1. 1885744666	-1. 2916831372
C	2. 6776226893	0. 5760680440	-0. 5781772567
H	4. 8043705350	-1. 2149816705	-0. 5993941502
H	4. 8225115648	-3. 4592890615	0. 4436057036
H	2. 7503704492	-4. 2618242332	1. 6429532484
H	0. 7622993337	-2. 7608242917	1. 7083047456
H	2. 1687041422	4. 1606857320	-1. 8659933338
H	4. 3479118764	2. 9720418794	-2. 3204360291
H	4. 6454386403	0. 6613198529	-1. 4775130625
H	0. 4014662786	2. 9579587183	-0. 5968820181
H	0. 2723646876	0. 3085405061	2. 5048343116

H	-0.2723646876	-0.3085405061	2.5048343116
---	---------------	---------------	--------------

Table S4. Crystal data and structure refinement for Rh(bpy)₂ClO₄

Identification code	rhbpypcor
Empirical formula	C ₂₄ H ₂₂ Cl N ₆ O ₄ Rh
Formula weight	1193.67
Temperature	153(2) K
Wavelength	0.95600 Å
Crystal system	Monoclinic
Space group	P2 ₁ /a
Unit cell dimensions	a = 24.952(14) Å α = 90.00(2) deg. b = 7.278(2) Å β = 115.82(2) deg. c = 28.858(25) Å γ = 90.00(3) deg.
Volume	4714.6(14) Å ³
Z	8
Density (calculated)	1.682 Mg/m ³
Absorption coefficient	0.868 mm ⁻¹
F(000)	2082
Crystal size	0.25 x 0.10 x 0.02 mm
Theta range for data collection	6.24 to 34.23 deg.
Index ranges	-29 ≤ h ≤ 26, 0 ≤ k ≤ 5, 0 ≤ l ≤ 33
Reflections collected	5030
Independent reflections	5030 [R(int) = 0.0000]
Refinement method	Full-matrix least-squares on F ²
Data / restraints / parameters	5030 / 0 / 349
Goodness-of-fit on F ²	1.065
Final R indices [I > 2σ(I)]	R1 = 0.1566, wR2 = 0.4335
R indices (all data)	R1 = 0.2280, wR2 = 0.4822
Largest diff. peak and hole	1.806 and -1.930 e.Å ⁻³

Table S5. Calculated bond lengths [\AA] and angles [degree] for $\text{Rh}(\text{H})_2(\text{bpy})_2^+$ and the transition-state complex

	$\text{Rh}(\text{H})_2(\text{bpy})_2^+$ in gas phase (B3LYP)	$\text{Rh}(\text{H})_2(\text{bpy})_2^+$ in methanol (B3LYP)	$\text{Rh}(\text{H})_2(\text{bpy})_2^+$ in gas phase (MP2)	Transition-state complex in gas phase (B3LYP)	Transition-state complex in methanol (B3LYP)	Transition-state complex in gas phase (MP2)
Rh–H	1.550	1.553	1.537	1.887	1.866	1.915
H–H	2.034	2.109	1.992	0.817	0.823	0.810
Rh–N	2.064, 2.235	2.081, 2.226	2.028, 2.179	2.053, 2.172	2.068, 2.196	2.009, 2.072
N–C2	1.363, 1.355	1.362, 1.357	1.360, 1.369	1.365, 1.361	1.365, 1.361	1.372, 1.372
C2–C3	1.403, 1.405	1.400, 1.401	1.406, 1.407	1.404, 1.405	1.401, 1.401	1.407, 1.407
C3–C4	1.396, 1.397	1.393, 1.394	1.400, 1.398	1.395, 1.395	1.392, 1.392	1.396, 1.397
C4–C5	1.399, 1.400	1.395, 1.396	1.403, 1.404	1.402, 1.402	1.397, 1.397	1.407, 1.406
C5–C6	1.395, 1.398	1.391, 1.394	1.398, 1.400	1.393, 1.395	1.390, 1.391	1.395, 1.395
C6–N	1.349, 1.341	1.349, 1.341	1.356, 1.348	1.351, 1.347	1.349, 1.346	1.361, 1.361
C2–C2'	1.487	1.483	1.481	1.475	1.475	1.465
H–Rh–H	82.1	85.5	80.8	25.0	25.5	24.4
H–Rh–N	94.7, 170.7, 86.4, 92.7	94.1, 169.2, 85.2, 87.5	96.1, 172.9, 95.1, 86.5	92.3, 129.6, 90.3, 104.9	92.7, 130.5, 90.7, 105.4	91.8, 127.4, 89.6, 103.2

N–Rh–N	77.3, 93.5, 101.7, 178.5	77.1, 100.6, 103.5, 179.1	78.4, 100.1, 87.8, 178.0	77.4, 101.4, 125.5, 177.3	76.9, 101.5, 124.1, 176.6	78.8, 129.4, 100.5, 178.5
Rh–N–C2	117.7, 112.7	117.1, 112.6	117.3, 113.1	117.8, 114.1	117.8, 113.9	117.3, 115.3
N–C2–C3	120.6, 121.2	120.4, 120.9	120.7, 121.1	120.7, 121.5	120.4, 121.2	121.0, 122.0
C2–C3–C4	120.0, 119.4	119.9, 119.3	120.0, 119.3	120.0, 119.6	119.9, 119.5	119.9, 119.7
C3–C4–C5	118.8, 119.0	119.1, 119.3	118.7, 119.1	118.8, 118.5	119.0, 118.9	118.7, 118.3
C4–C5–C6	118.6, 118.2	118.6, 118.4	119.0, 118.5	118.6, 118.7	118.6, 118.6	119.0, 119.2
C5–C6–N	120.7, 122.9	122.4, 122.6	122.3, 122.5	122.8, 123.2	122.6, 122.9	122.5, 123.1
C6–N–C2	119.4, 119.3	119.7, 119.6	119.3, 119.6	119.2, 118.5	119.4, 118.9	118.9, 117.7
C6–N–Rh	123.0, 127.9	123.1, 127.2	123.4, 127.3	123.0, 127.3	122.8, 127.2	123.6, 126.7
N–C2–C2'	116.6, 115.8	116.5, 116.0	116.0, 115.2	115.6, 115.1	115.9, 115.3	114.3, 114.0
C2'–C2–C3	122.8, 123.0	123.1, 123.2	123.2, 123.7	123.4, 123.8	123.5, 123.7	124.7, 124.0

Legends for Figures

Figure S1. Plot of rate constants for the formation of $\text{Rh}(\text{H})_2(\text{bpy})_2^+$ as a function of H_2 concentration in methanol at 25 °C

Figure S2. Eyring plots for the determination of ΔH^\ddagger and ΔS^\ddagger for reaction (1) in methanol: for the (a) forward reaction, and (b) reverse reaction.

Figure S3. Spectral changes recorded every 2 min for the reaction of $\text{IrCl}(\text{CO})(\text{PPh}_3)_2$ to form $\text{Ir}(\text{H})_2\text{Cl}(\text{CO})(\text{PPh}_3)_2$ under 1 atm H_2 and 35 °C.

Figure S4. Plots of $\ln(k_{\text{obs}})$ versus pressure for the oxidative addition of H_2 (black) and D_2 (red) to $\text{IrCl}(\text{CO})(\text{PPh}_3)_2$ in toluene.

Figure S5. X-ray structure of $\text{Rh}(\text{bpy})_2^+$: An ORTEP drawing showing the atom numbering (a) and a packing diagram (b) showing that the rhodium complexes are stacked in infinite chains along the crystallographic two-fold screw axis.

Figure S6. Two views of the transition-state complex for the oxidative addition of H_2 to $\text{Rh}(\text{bpy})_2^+$.

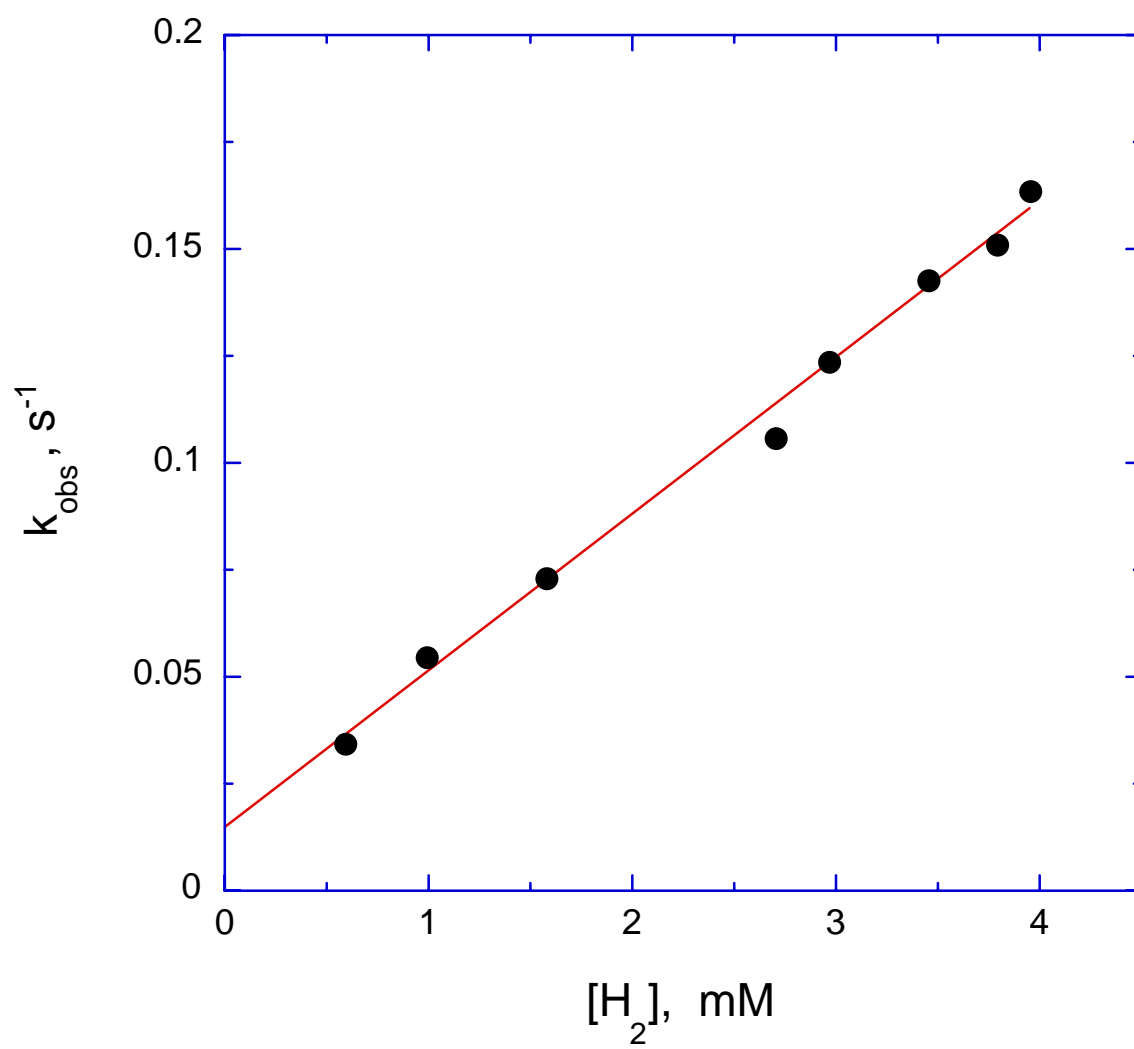


Figure S1.

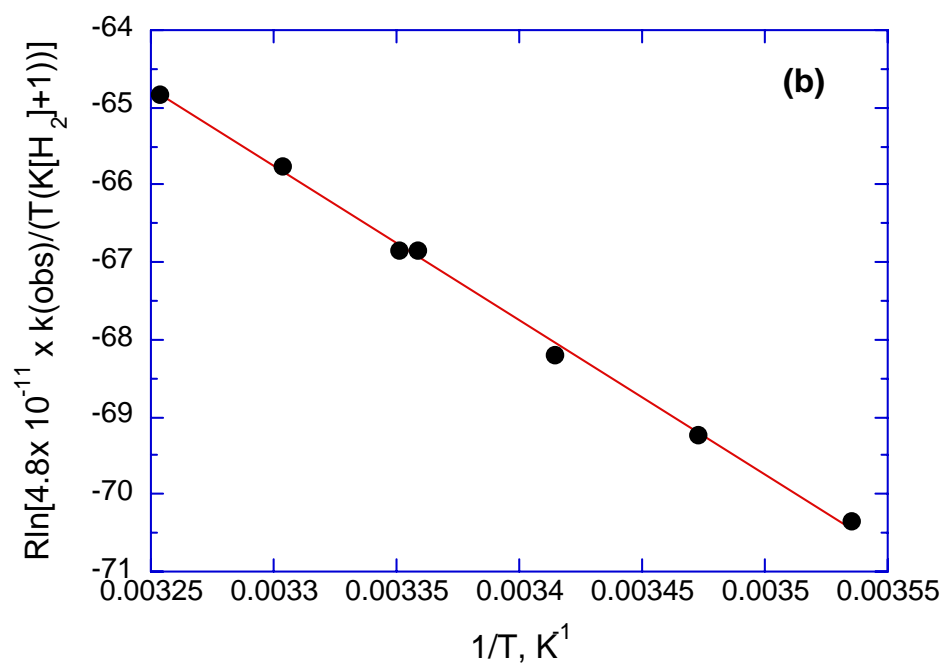
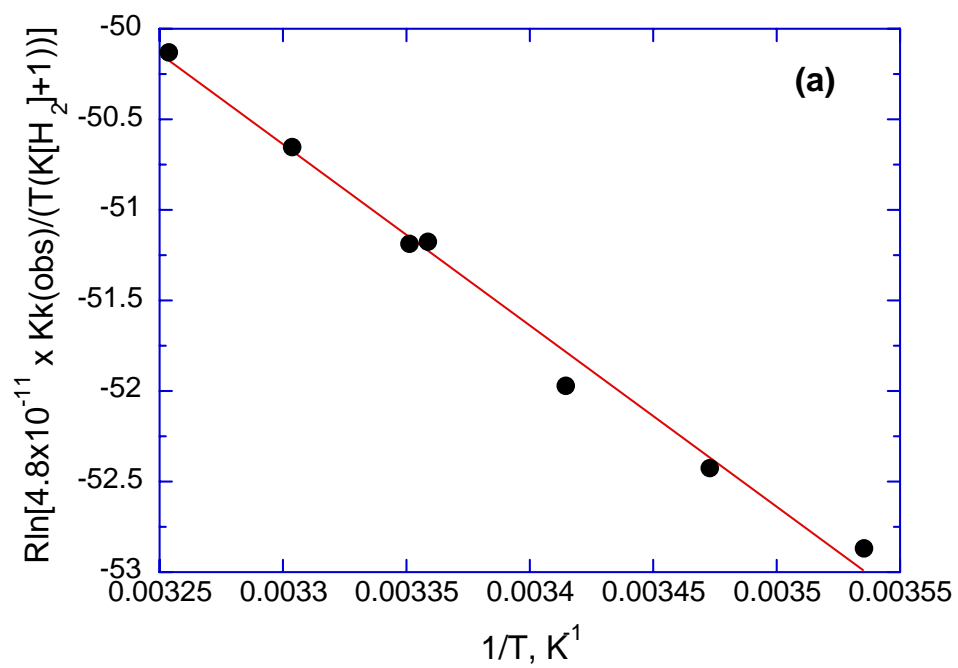


Figure S2.

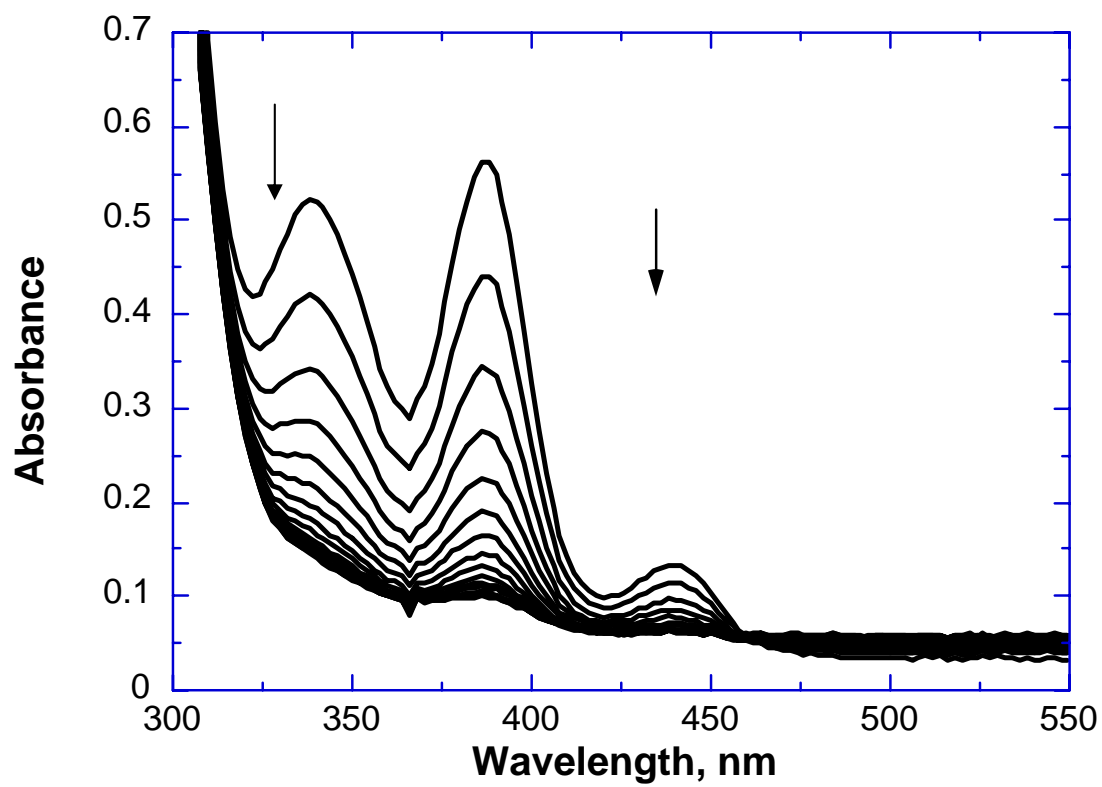


Figure S3.

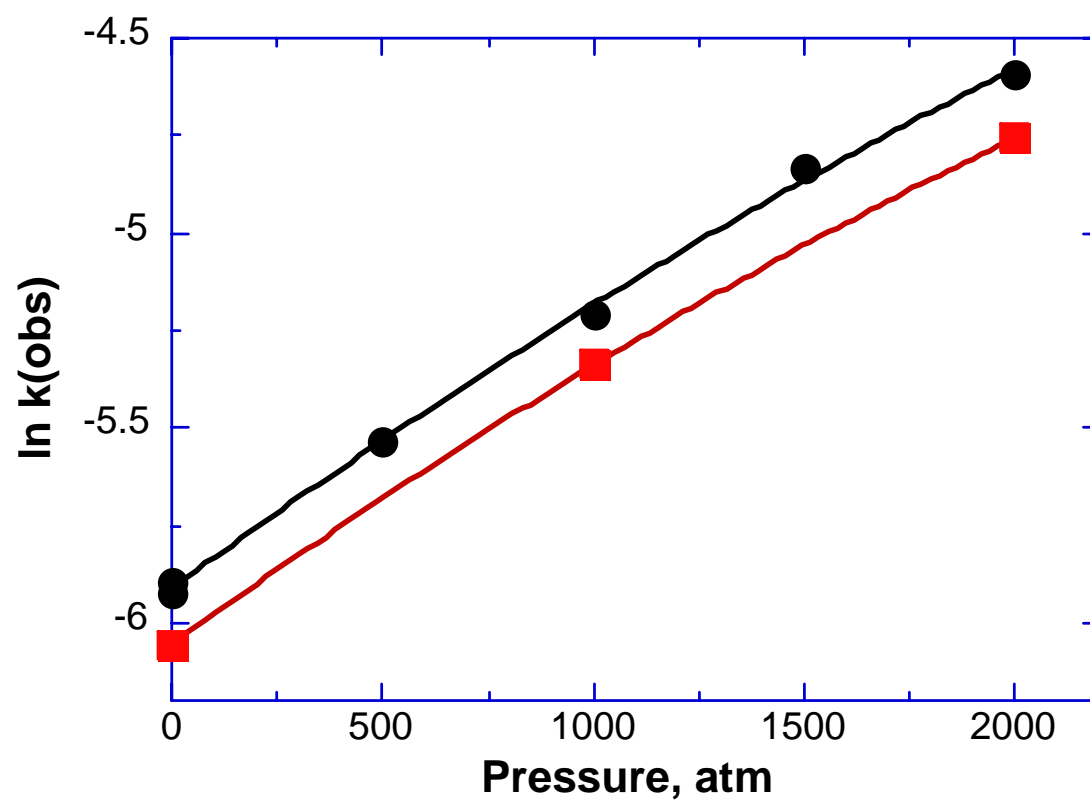


Figure S4.

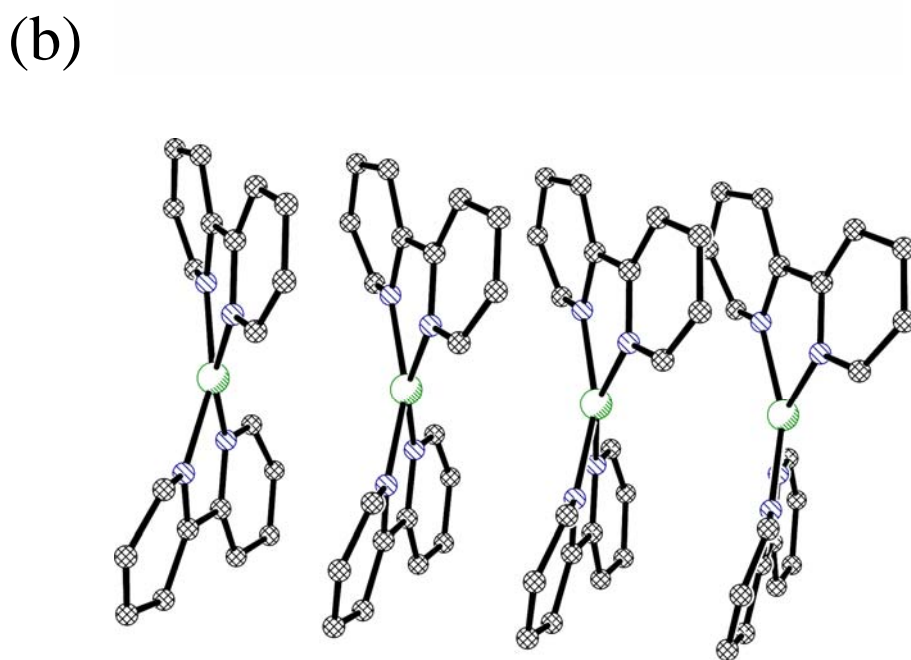
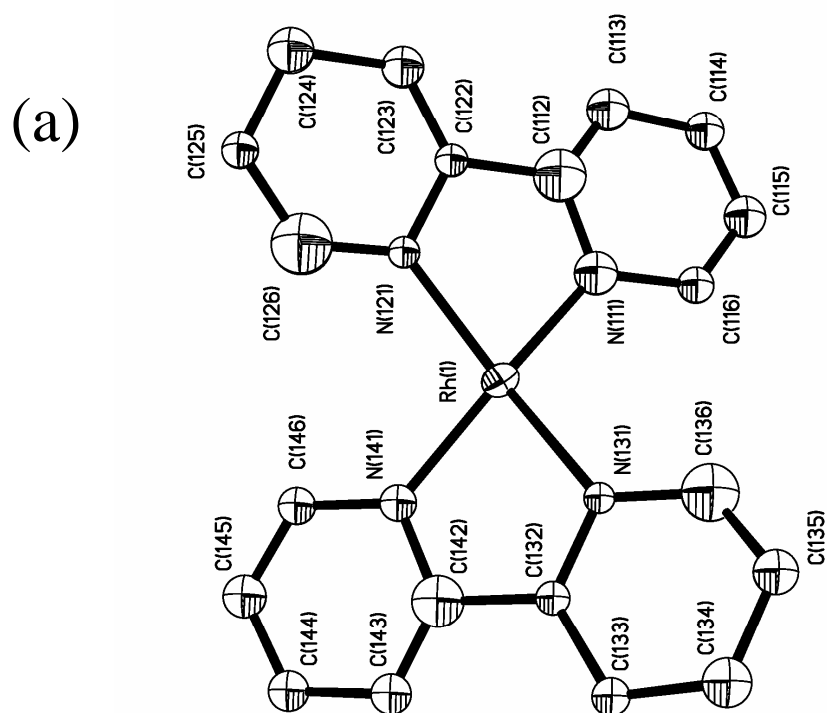


Figure S5.

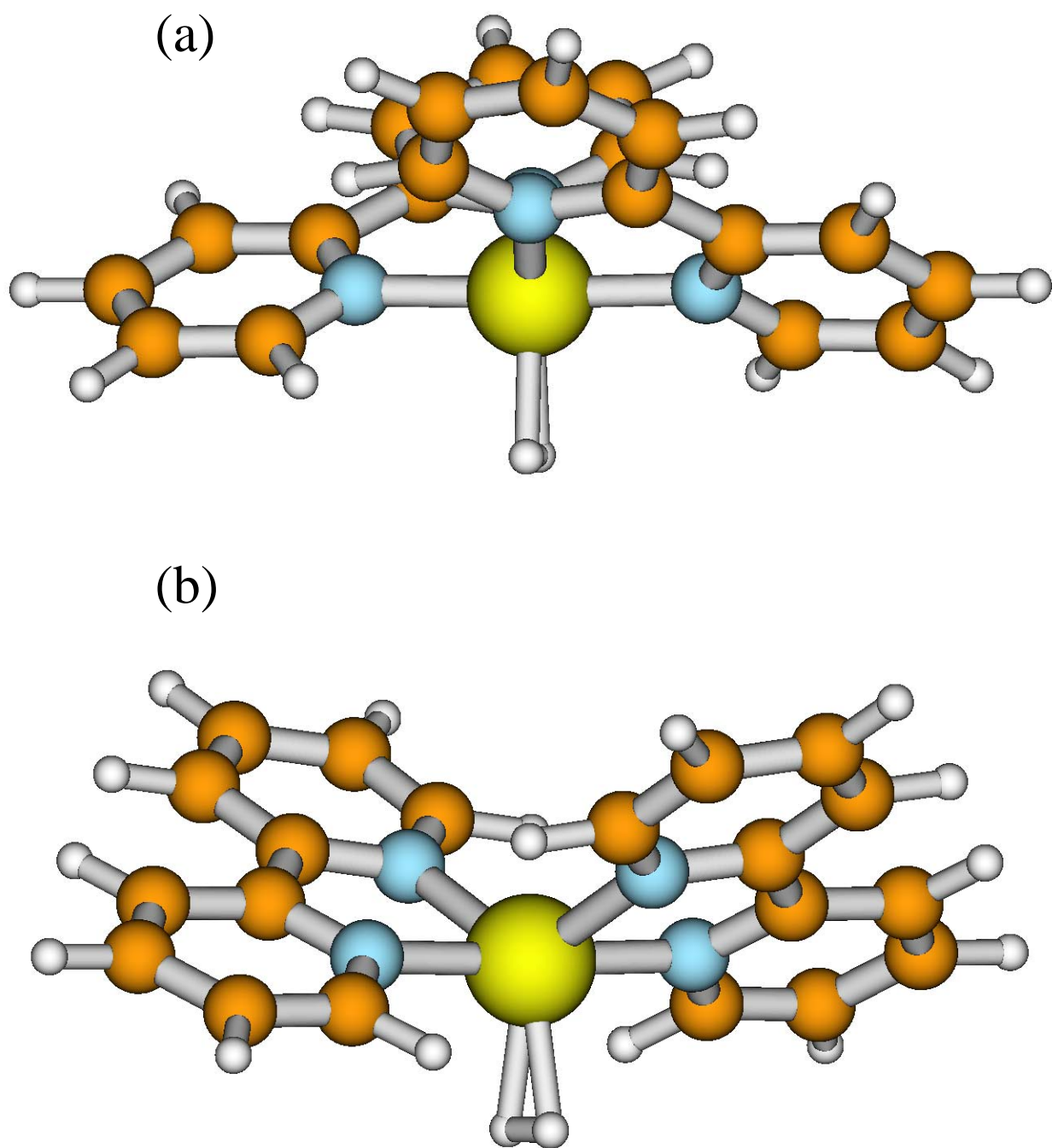


Figure S6.